Hindawi
Journal of Sensors
Volume 2021, Article ID 8883005, 9 pages
https://doi.org/10.1155/2021/8883005

Research Article

Improvement of the Communication between RFID Sensor Network Devices Used to Control and Monitor a Building

Abdelhamid Bou-El-Harmel, Ali Benbassou, and Jamal Belkadid

Laboratory of Innovative Technologies Eq. CEM/Telecoms Sidi Mohamed Ben Abdullah University, High School of Technology, Road IMOUZZER, BP 2427 Fez, Morocco

Correspondence should be addressed to Abdelhamid Bou-El-Harmel; abdelhamid.bouelharmel@usmba.ac.ma

Received 24 July 2020; Revised 5 January 2021; Accepted 10 January 2021; Published 29 January 2021

Academic Editor: Giorgio Pennazza

Copyright © 2021 Abdelhamid Bou-El-Harmel et al. This is an open access article distributed under the Creative Commons Attribution License, which permits unrestricted use, distribution, and reproduction in any medium, provided the original work is properly cited.

In the RFID sensor network (RSN), the devices communicate with each other by RF waves using the antennas through a propagation channel. A poor communication between these devices results in either a significant economic loss or security threats. The communication problems can have several origins depending on the type of antenna used and the nature of the propagation channel. In this work, our objective is to limit the communication problems between the nodes of this network that are linked to the characteristics of an indoor propagation channel. The goal is to predict the channel characteristics using the 3D ray tracing method in order to select the appropriate transmission parameters such as transmission power and duration of a symbol. To achieve this, we have modeled a building that is sectioned as a propagation channel where network devices are deployed for control and monitoring. The communication was made at 915 MHz using the quasi-isotropic 3D cubic antenna that we designed as well as a conventional dipole antenna in order to compare the results. We have found that the use of the 3D cubic antenna gives several advantages to the RFID sensor network compared to the most commonly used conventional dipole antenna, such as a transmission power of 0 dBm which automatically leads to an increase in the lifetime of the devices, as well as a minimum symbol duration of around 219.78 ns which gives a high bit rate.

1. Introduction

The RSN network is a new research field for industrialists and academics. It combines the properties of RFID technology to WSN technology and vice versa [1, 2]. This association makes it possible to extend the operational and functional capabilities of the devices in order to respond to the needs of the applications.

In RSN applications, the devices communicate with each other by RF waves using the antennas through a propagation channel. A poor communication between these devices results in either a significant economic loss or security threats. The communication problems can have several origins depending on the type of antenna used and the nature of the propagation channel.

The antennas are fundamental and essential elements in communication between devices of the RSN network. Each antenna has different radiation characteristics. The most commonly used antennas are dipoles and monopoles [3, 4]. The latter produce radiation in the form of a doughnut with zero field strength areas along their axis. In these areas, poor communication occurs between network nodes.

In order to ensure reliable communication between RSN nodes at the antennas level, we have designed in previous work new antennas in 3D form that produce quasi-isotropic radiation, such as the cubic [5, 6] and spherical [7] antennas.

Regarding the propagation channel, it corresponds to the environment traversed by the RF waves during the transmission of information between the transmitting and receiving antennas of the nodes of the RSN network. Most RSN applications are deployed inside buildings, which constitutes a multipath propagation channel. These multiple paths can generate destructive interference at the receiving node which produces a fading of the received signal. Thus, the long propagation delays between the different paths and their variation

Figure 1: A view of the building taken by Google Maps.

with time can cause intersymbol interference (ISI) and symbol estimation errors (SEE), respectively. All of these problems contribute to poor RF transmission between network nodes.

A good transmission then requires a good choice of transmission parameters such as the transmission power P_t and the symbol duration T_s. These parameters are directly linked to the characteristics of the propagation channel, i.e., received power P_r, coherence band B_c, and coherence time T_c.

In previous work [8], we have studied the effects of the orientation of two different antennas on the characteristics of the multipath propagation channel in a typical indoor environment. The propagation channel characteristics are compared in terms of received power level (P_r) and delay spread (τ_{RMS}) for the 3D cubic antenna and the conventional dipole in the LOS, NLOS, and OLOS scenarios.

In this work, our objective is to predict the appropriate transmission parameters (P_t and T_s) using our 3D cubic antenna and the conventional dipole antenna as transmitting and receiving antenna of the RSN network and to compare the results obtained. For this purpose, we will in "Environment, Location, and Antennas" model the indoor environment (building) that has been selected as the propagation channel where the RSN network will be deployed, as well as specify the location of the nodes and determine the antennas used with their radiation characteristics. In "3D Ray Tracing Method", we will present the 3D ray tracing method. In "Results and Analysis", we will present the predicted propagation channel characteristics as well as the appropriate transmission parameters with a comparison between the results obtained.

2. Environment, Location, and Antennas

2.1. Selected Environment. The selected environment as the propagation channel where the RSN network is deployed is the one we have already modeled in the work [8]. We remind that this environment is a building within our university [9] (see Figure 1).

The complete modeling of this two-floor building is very complex. We were only interested in modeling the north wing of the first floor (see Figure 2) where our laboratory is

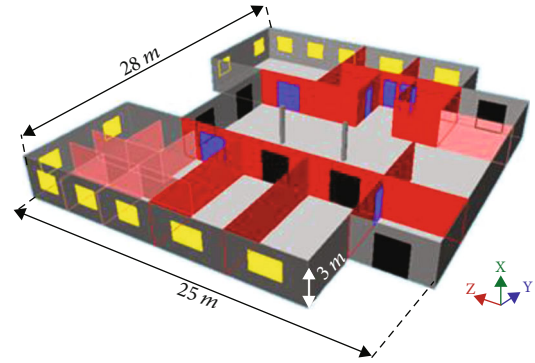

Figure 2: First floor of the north wing of the building in 3D.

Table 1: Dielectric constants of materials.

Types	$\varepsilon_r = \varepsilon_r' + j\varepsilon_r''$	
	ε_r'	ε_r''
Reinforced-concrete wall	6.7	−1.2
Brick wall	5.1	−0.2
Glass partition	5	0
Iron door	1	0
Wood door	3	0
Glass window	5	0
Ground	10	−1.2
Roof	10	−1.2

located. This floor consists of reinforced-concrete and brick walls, glass partitions, iron and wooden doors, and glass windows.

All the constituents of our environment are considered homogeneous and having complex dielectric constants (see Table 1) obtained from a free space method using transmission measurements at normal incidence [10]. Obstacles such as cupboards, machines, and desks are not modeled because of the complexity of their design.

2.2. Location of RSN Nodes. The RSN network is used for control and monitoring of the building with a star topology, as shown in Figure 3. The terminal nodes are deployed and fixed above the doors and windows with a height from the ground of 2.5 m. This position is most optimal for integrating several types of sensors (motion sensor, temperature sensor, gas sensor, camera, etc.) with the magnetic contact sensor which is used to monitor the opening and closing of doors and windows. All detected information is transmitted to the coordinator node which is located in the middle of the corridor with a height above the ground of 2.5 m. In the star topology, the network is controlled by the coordinator node, so we choose it as a transmitter (Tx) and the terminal nodes as receivers (Rx).

2.3. Used Antennas. In this study, we use, for RF communication between the nodes of the network, the 3D cubic antenna that we designed and the conventional half-wave dipole antenna. We remind that the 3D cubic antenna produces a

quasi-isotropic radiation pattern with a maximum gain of 1.29 dBi and circular polarization; on the other hand, the dipole antenna produces a radiation in the form of a doughnut with a maximum gain of 2.14 dBi and a polarization linear. The position of these two antennas relative to the environment is shown in Figure 4.

During communication, the frequency and power of transmission used are, respectively $f = 915$ MHz (the resonant frequency of the two antennas) and $P_t = 0$ dBm (the minimum transmission power of the RSN devices).

2.4. 3D Ray Tracing Method. The 3D ray tracing method is an asymptotic method based on the following:

(i) The Geometric Optics (GO) method [11] to describe the direct, reflected and transmitted fields by the concept of rays, as shown in Figure 5(a)

(ii) The Uniform Diffraction Theory (UDT) [12] to describe the diffracted fields by the concept of rays (see Figure 5(b)).

To identify the rays (paths) that propagate between the antennas, the RT-3D method uses the image method and the folding method [13]. The implementation of the RT-3D method is very complex but offers a complete description of the received waves [14]. Once all propagation rays are determined, the received power in dB is calculated by [15]:

$$P_r[dB] = 10 \log \left(\frac{|E_{tot}|^2}{\eta_0} A \right), \quad (1)$$

where

(i) $\eta_0 = \sqrt{\mu_0/\epsilon_0} = 120\pi$ is the intrinsic impedance of air with μ_0 and ϵ_0 being the permeability and permittivity of the vacuum, respectively

(ii) $A = (\lambda^2 G_r/4\pi)$ is the effective area of the receiving antenna with λ being the wavelength and G_r the gain of the receiving antenna

(iii) $E_{tot} = \sum_i E_i$ is the combination of the direct field between the Tx node and the Rx node, the fields reflected by obstacles, the fields transmitted through obstacles, and the fields diffracted by the edges of obstacles. With

$$E_i = \frac{E_0 f_t f_r e^{-jkd_i}}{d_i} \prod_{a=1}^{n} \mathrm{R}_a \prod_{b=1}^{m} T_b \prod_{c=1}^{l} D_c, \quad (2)$$

where

(i) $E_0 = P_t G_e/4\pi$ is the reference field

(ii) f_t and f_r are the characteristic functions of the radiation in the ray direction between transmitting and receiving antennas, respectively

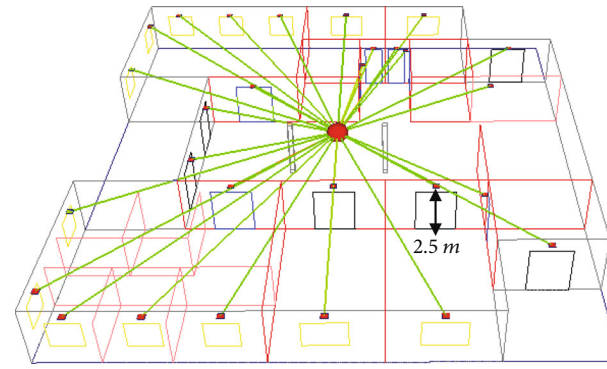

Figure 3: Location of the nodes of the RSN network according to the star topology.

(iii) $k = 2\pi/\lambda$ is the constant of propagation

(iv) d_i is the length of path i

(v) n, m, and l are the total numbers of reflections, transmissions, and diffractions, respectively

(vi) R_a, T_b, and D_c are the reflection coefficient of the a^{th} reflection, the transmission coefficient for the b^{th} transmission, and the diffraction coefficient for the c^{th} diffraction, respectively.

During the simulation, the maximum number of reflections, transmissions, and diffractions is in the order of 5. The receivers of the RSN node are capable of achieving a sensitivity between −92 dBm and −107.5 dBm [16, 17]. Therefore, we will choose the −92 dBm value as the sensitivity threshold of the *Rx*.

3. Results and Analysis

3.1. Received Power. After the simulations, Figure 6 presents the prediction results of the received power P_r[dBm] at each *Rx* using the two antennas ((a) 3D cubic and (b) dipole). According to the results, we observe that the received power P_r varies randomly as a function of the distance between *Tx* and each *Rx*, which is due to the different paths received at each *Rx*.

When using the 3D cubic antenna, we have obtained a minimum power value of −77.35 dBm at distance 14.03 m. However, during the use of the conventional dipole antenna, the minimum value of the power is −74.18 dBm at the distance of 14.44 m.

In this study, we have positioned the 3D cubic antenna of the RSN nodes in the same way throughout the environment. The orientation of the antennas relative to each other changes the values of the power P_r as we have found in the work [8]. Table 2 summarizes the maximum differences between the levels of the power P_r obtained during all the orientations of the 3D cubic and dipole antennas in the LOS, NLOS, and OLOS scenarios.

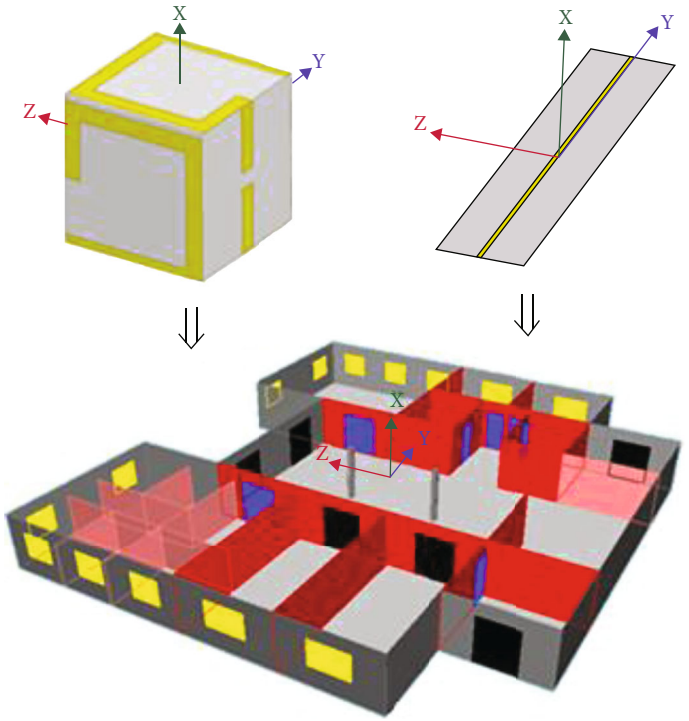

Figure 4: Position of the antennas in relation to the environment.

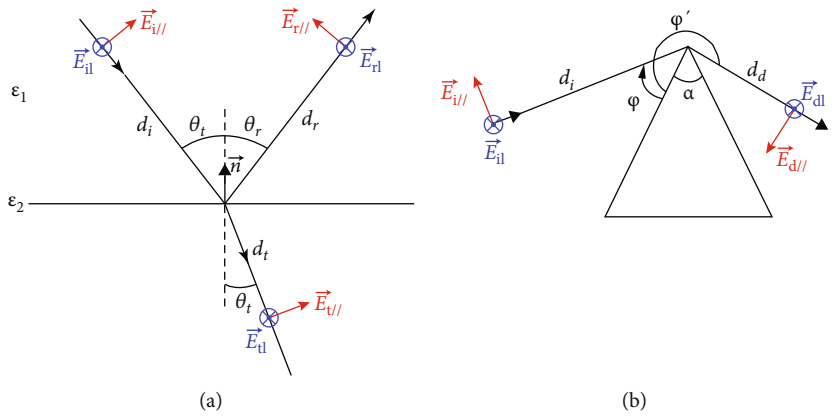

Figure 5: (a) Reflection and transmission of an incident wave and (b) diffraction of an incident wave.

As shown in Table 2, the two maximum power differences obtained when orienting the 3D cubic antenna and the dipole antenna are 6.85 dBm and 27.97 dBm, respectively. Therefore, the minimum value of the power obtained when using the 3D cubic antenna becomes −84.2 dBm and when using the dipole antenna becomes −102.15 dBm.

As regards the fight against the fading of the received signal, the minimum value of the power P_r must be greater than the sensitivity threshold 4of the *Rx* (−92 dBm). This implies that the value of the transmission power P_t (0 dBm) chosen at the outset is satisfactory to ensure reliable RF transmission between the nodes of the RSN network using the 3D cubic antenna. On the contrary, the power P_t must be increased when using the dipole antenna, which will decrease the lifespan of the devices.

3.2. Coherence Band. The coherence band B_c is obtained from the maximum delay T_m by the following relation:

$$B_c = \frac{1}{T_m}, \tag{3}$$

with T_m being the delay between the first and last pulse of the impulse response (IR) of each channel, as shown in Figure 7 which represents three predicted IRs at the level of three *Rx* using the 3D cubic antenna.

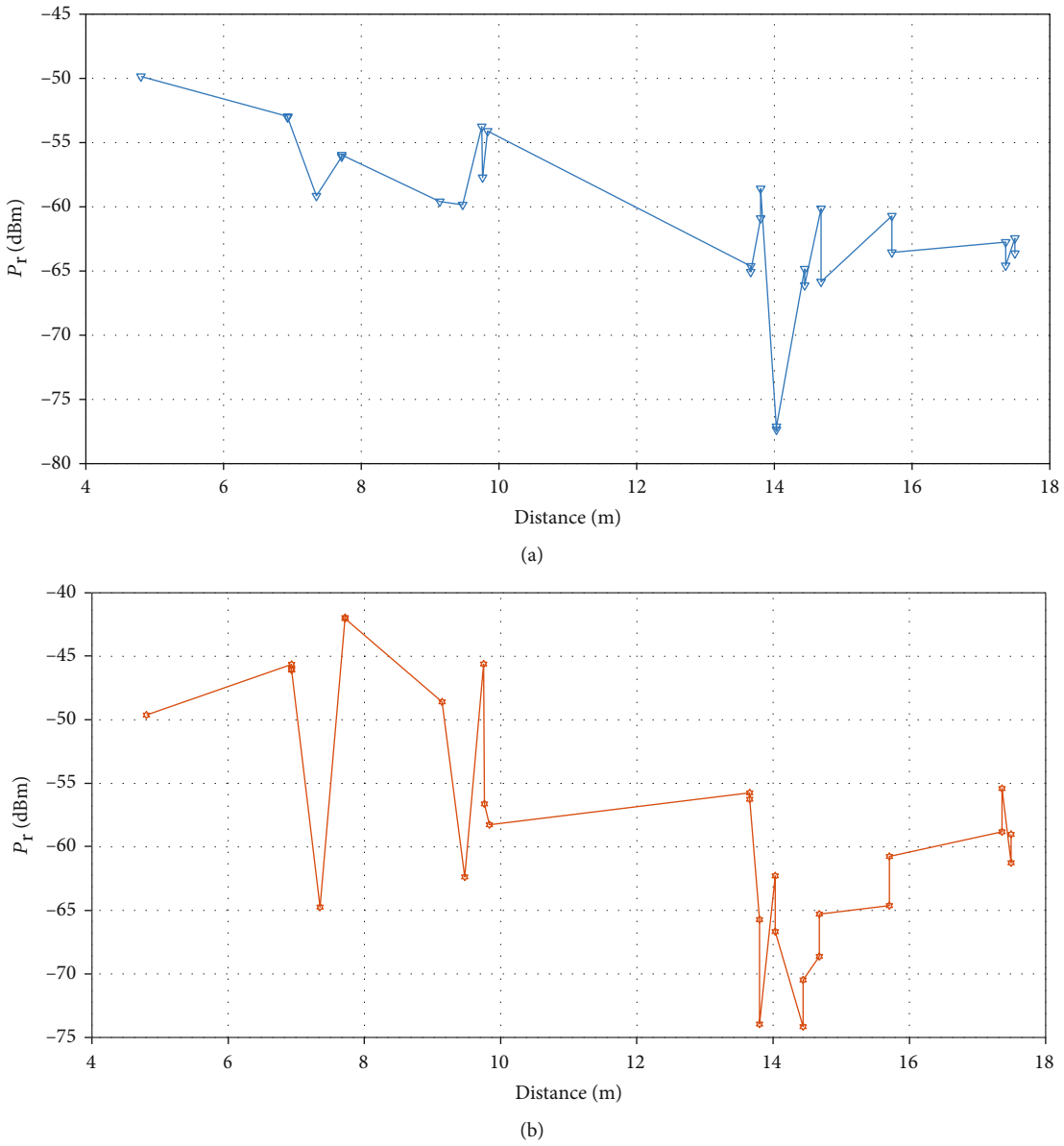

Figure 6: P_r predicted as a function of the distance between Tx and each Rx when using (a) the 3D cubic antenna and (d) the dipole antenna.

Table 2: Maximum differences between the levels of the P_r during the orientations of the 3D cubic and dipole antennas [8].

Scenarios	3D cubic antenna	Dipole antenna
LOS	6.85 dBm	27.81 dBm
NLOS	6.07 dBm	25.08 dBm
OLOS	4.6 dBm	27.97 dBm

In the case where the transmission power P_t is insufficient, the increase of this one leads to an increase in the number of paths received, which implies an increase in the values of the delay T_m. Therefore, we will use the delay dispersion τ_{RMS} which takes into account the importance of the paths in order to calculate the coherence band:

$$\tau_{\text{RMS}} = \sqrt{\frac{\sum_i P_i \tau_i^2}{\sum_i P_i} - \left[\frac{\sum_i P_i \tau_i}{\sum_i P_i}\right]^2}. \quad (4)$$

The relationship between the coherence band B_c and the delay spread τ_{RMS} has been proposed by [18] as follows:

$$B_c \approx \frac{1}{\alpha \tau_{\text{RMS}}}, \quad (5)$$

where α is a coefficient that depends on the nature of the propagation channel. In work [19], the authors found that $\alpha = 1/0.15$ in an indoor radio channel.

Figure 8 displays the levels of τ_{RMS} as a function of the distance between the Tx and each Rx when using the two antennas ((a) 3D cubic and (b) dipole).

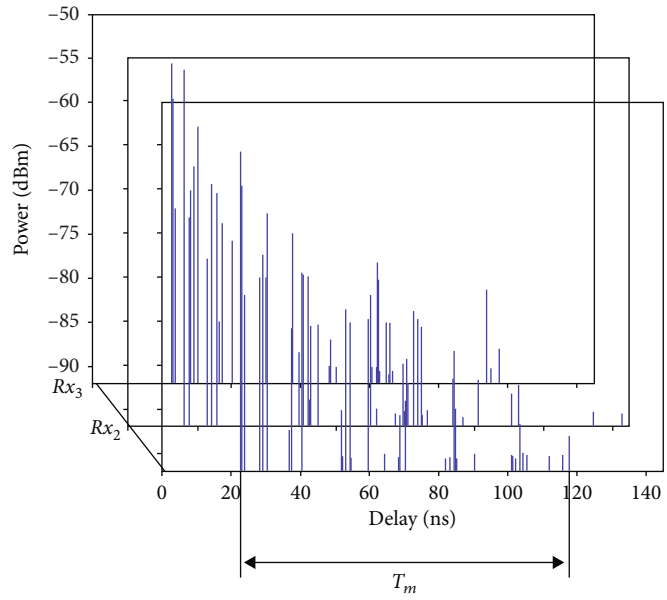

Figure 7: Impulse responses (IRs) at the level of three *Rx* using the 3D cubic antenna.

According to the results and when using the 3D cubic antenna, we have obtained a maximum value of τ_{RMS} of 23.66 ns at a distance 14.03 m. On the other hand, the maximum value of the τ_{RMS} obtained when using the conventional dipole antenna is 39.76 ns at the same distance.

The values of τ_{RMS} change depending on the orientation of the antennas as we have shown in the work [8]. Table 3 summarizes the maximum differences between the levels of τ_{RMS} obtained during all orientations of the 3D cubic and dipole antennas in the LOS, NLOS, and OLOS scenarios.

According to the table, the two maximum differences of τ_{RMS} obtained when orienting the 3D cube antenna and the dipole antenna are 9.34 ns and 28.49 ns, respectively. Therefore, the maximum value of τ_{RMS} obtained when using the 3D cube antenna becomes 33 ns and when using the dipole antenna becomes 68.25 ns.

Then, the minimum value of B_c obtained using the 3D cubic antenna and the conventional dipole antenna are 4.55 MHz and 2.2 MHz, respectively. Therefore, the signal bandwidth B_s must be lower than the coherence band B_c in order to limit intersymbol interference (ISI).

For digital modulation, the B_s is calculated from the symbol duration T_s by

$$B_s = \frac{1}{T_s}. \tag{6}$$

So, to limit ISI, the T_s duration must be greater than 219.78 ns when using the 3D cubic antenna. On the other hand, the T_s duration must be greater than 454.55 ns when using the conventional dipole antenna.

3.3. Coherence Time. To limit symbol estimation errors (SEE), the duration T_s must be less than the coherence time T_c resulting from the mobility of network nodes and obstacles. In our case, the nodes are fixed, and the obstacles that are always moving are humans. The influence of obstacle mobility is very negligible compared to that of node mobility.

Consequently, we can consider that the human wears nodes, in order to know only the maximum value of the duration T_s that we will not exceed. From Equation (7), we can plot the variation of T_c (see Figure 9) as a function of the human speed V, which normally does not exceed 1 m/s.

$$T_c \approx \frac{9}{16\pi f(V/C)}. \tag{7}$$

According to the results, the minimum T_c is 6.52 ms, which implies that the duration T_s must be less than this value in order to limit SEE.

To conclude, the duration T_s must be between 219.78 ns and 6.52 ms to limit ISI and EES during the use of the 3D cubic antenna. On the other hand, it must be between 454.55 ns and 6.52 ms when using the conventional dipole antenna.

The limit of duration T_s also limits the bit rate D because D is the product of the inverse of T_s (modulation rate R) and the logarithm to the base 2 of the number of possible states of a symbol (valence V) [20]:

$$D = \frac{1}{T_s}\ \log_2(V). \tag{8}$$

Tables 4 and 5 list the limiting values of D as a function of V when using the 3D cubic antenna and the conventional dipole antenna, respectively.

Usually, the bit rate D must be high to ensure low data transfer time. Therefore, the duration T_s must be chosen close to the minimum value. This implies that we will not have SEE whatever the movement of nodes and obstacles.

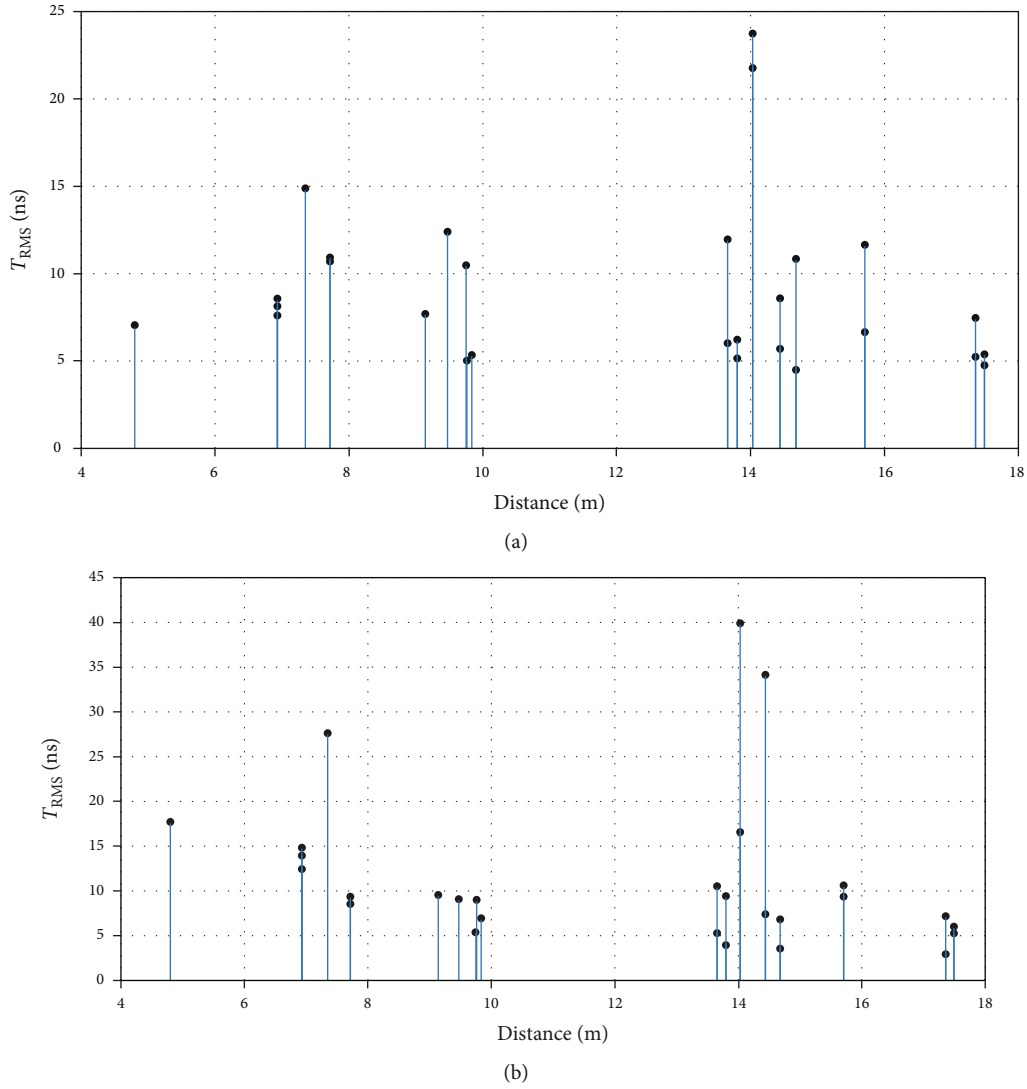

Figure 8: Dispersion of delays τ_{RMS} as a function of the distance between Tx and each Rx using the antenna: (a) 3D cubic and (b) dipole.

Table 3: Maximum deviations between the levels of τ_{RMS} during the orientations of the 3D cubic and dipole antennas [8].

Scenarios	3D cubic antenna	Dipole antenna
LOS	6.48 ns	28.49 ns
NLOS	4.64 ns	23.62 ns
OLOS	9.34 ns	27.97 ns

From both Tables 4 and 5, we have a very high bit rate when using the 3D cubic antenna compared to using the conventional dipole antenna. Then, the use of our 3D cubic antenna is better than the conventional dipole antenna.

4. Conclusions

In this work, we have modeled a building that has been selected as a propagation channel where the RSN network is deployed for control and monitoring. For the transmission, we have used the 3D cubic antenna that we have designed and the conventional dipole antenna which is the most used in the RSN network. By means of the 3D ray tracing method, we have predicted the characteristics of the propagation channel in order to improve the communication between the devices of the RSN network in terms of the appropriate transmission parameters such as the transmission power P_t and the duration of a symbol T_s. We have found as results to fight against fading of the received signal that a transmission power of 0 dBm is sufficient when using our 3D cube antenna. However, it is necessary to increase this power during the use of the conventional dipole antenna, which automatically leads to a decrease in the lifetime of the devices, which is a disadvantage. To limit ISI and EES, the symbol duration must be close to a minimum value of the order of 219.78 ns when using our 3D cubic antenna and of the order of 454.55 ns when using the conventional dipole antenna. These two values result in different bit rates. The use of our

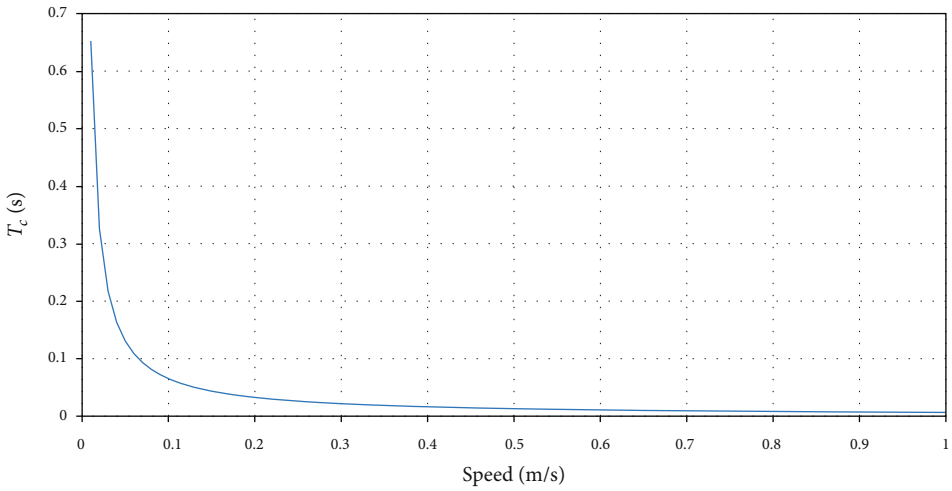

Figure 9: Coherence time T_c as a function of speed V.

Table 4: Limiting values of bit rate D as a function of valence V when using the 3D cubic antenna.

Minimum value	Parameters	Maximum value
153.37 bit/s <	$D(V=2)$	<4.55 Mbit/s
306.75 bit/s <	$D(V=4)$	<9.1 Mbit/s
460.12 bit/s <	$D(V=8)$	<13.65 Mbit/s

Table 5: Limiting values of bit rate D as a function of valence V when using the conventional dipole antenna.

Minimum value	Parameters	Maximum value
153.37 bit/s <	$D(V=2)$	<2.2 Kbit/s
306.75 bit/s<	$D(V=4)$	<4.4 Mbit/s
460.12 bit/s<	$D(V=8)$	<6.6 Mbit/s

antenna provides a high bit rate in order to ensure a low data transfer time. To conclude, our antenna gives several advantages for the RFID sensor array compared to the most commonly used antennas.

Data Availability

Requests for access to data should be made to Abdelhamid BOU-EL-HARMEL,
abdelhamid.bouelharmel@usmba.ac.ma.

Conflicts of Interest

The authors declare that there is no conflict of interest regarding the publication of this paper.

References

[1] S. Mejjaouli and R. F. Babiceanu, "RFID-wireless sensor networks integration: decision models and optimization of logistics systems operations," *Journal of Manufacturing Systems*, vol. 35, pp. 234–245, 2015.

[2] A. Mitrokotsa and C. Douligeris, "Integrated RFID and sensor networks: architectures and applications," *RFID and Sensor Networks: Architectures, Protocols, Security and Integrations*, vol. 512, pp. 511–535, 2009.

[3] R. C. Hadarig, M. E. de Cos, and F. Las-Heras, "UHF dipole-AMC combination for RFID applications," *IEEE Antennas and Wireless Propagation Letters*, vol. 12, pp. 1041–1044, 2013.

[4] A. E. Abdulhadi and R. Abhari, "Design and experimental evaluation of miniaturized monopole UHF RFID tag antennas," *IEEE Antennas and Wireless Propagation Letters*, vol. 11, pp. 248–251, 2012.

[5] A. Bou-El-Harmel, A. Benbassou, and J. Belkadid, "Design of a three-dimensional antenna UHF in the form cubic intended for RFID, wireless sensor networks (WSNs) and RFID sensor networks (RSNs) applications," *International Journal on Communications Antenna and Propagation (IRECAP)*, vol. 4, no. 6, pp. 260–264, 2014.

[6] A. Bou-El-Harmel, A. Benbassou, and J. Belkadid, "Optimization of a 3D UHF cubic antenna with quasi-isotropic radiation pattern for RFID, WSN and RSN applications," *WSEAS Transactions on Communications*, vol. 14, pp. 365–373, 2015.

[7] A. Bou-El-Harmel, A. Benbassou, and J. Belkadid, "Design and development of a new electrically small 3D UHF spherical antenna with 360° of opening angle in the whole space for RFID, WSN, and RSN applications," *International Journal of Antennas and Propagation*, vol. 2016, Article ID 2906149, 18 pages, 2016.

[8] A. Bou-El-Harmel, A. Benbassou, J. Belkadid, and N. Mechatte, "Effect of quasi-isotropic antenna orientation on indoor multipath propagation characteristics in RSN applications," *International Journal of Antennas and Propagation*, vol. 2017, Article ID 2686123, 13 pages, 2017.

[9] "La cité de l'innovation," http://www.usmba.ac.ma/~citt/.

[10] C.-F. Yang, C.-J. Ko, and B.-C. Wu, "A free space approach for extracting the equivalent dielectric constants of the walls in buildings," in *IEEE Antennas and Propagation Society International Symposium*, pp. 1036–1039, Baltimore, MD, USA, July 1996.

[11] O. N. Stavroudis, *The Mathematics of Geometrical and Physical Optics*, John Wiley & Sons, 2006.

[12] J. Russell and R. Cohn, *Uniform Theory of Diffraction*, Book on Demand, 2012.

[13] L. Aveneau, Y. Pousset, R. Vauzelle, and M. Mériaux, "Development and evaluations of physical and computer optimizations for the 3D UTD model," in *AP2000 Millennium Conference on Antennas & Propagation*, pp. 9–14, Davos, Switzerland, 2000.

[14] G. E. Athanasiadou and A. R. Nix, "A novel 3-d indoor ray-tracing propagation model: the path generator and evaluation of narrow-band and wide-band predictions," *IEEE Transaction on Vehicular Technology*, vol. 49, no. 4, pp. 1152–1168, 2000.

[15] Z.-Y. Liu, L.-X. Guo, and X. Meng, "Efficient three-dimensional ray-tracing model for electromagnetic propagation prediction in complex indoor environments," *The Journal of the Optical Society of America A*, vol. 30, no. 8, p. 1654, 2013.

[16] A. Bildea, *Link Quality in Wireless Sensor Networks*, HAL, 2015.

[17] Analog Devices, *Analog Devices Wireless Sensor Network (WSN) Solutions*, Analog devices, 2014, Project Code: APM-WSN-2014.

[18] M. J. Gans, "A power-spectral theory of propagation in the mobile-radio environment," *IEEE Transactions on Vehicular Technology*, vol. 21, no. 1, pp. 27–38, 1972.

[19] K. Pahlavan and S. J. Howard, "Frequency domain measurements of indoor radio channels," *Electronics Letters*, vol. 25, no. 24, pp. 1645–1647, 1989.

[20] D. Dromard and D. Seret, *Architecture des réseaux*, Pearson Education France, 2013.